BRNO UNIVERSITY OF TECHNOLOGY

Faculty of Electrical Engineering and Communication

Ing. Vojtěch SVOBODA

THE INFLUENCE OF FAST CHARGING ON THE PERFORMANCE OF VRLA BATTERIES

VLIV RYCHLÉHO NABÍJENÍ NA FUNKČNÍ CHARAKTERISTIKY VRLA BATERIÍ

SHORT VERSION OF PHD THESIS

Study Field: Microelectronics and Technology

Supervisor: Doc. RNDr. Miroslav Cenek, CSc.

Opponents: Prof. Dr. Jürgen Garche   (ZSW Ulm)
                  Doc. Ing. Jiří Vondrák, DrSc.   (AV ČR)
                  Ing. Jiří Mrha, DrSc.

Presentation Date: 17. 12. 2002

KEY WORDS

lead-acid battery, VRLA, fast charging, current step down fast charge, cycle life, current distribution, electrolyte stratification, irreversible sulfation, grid and spines corrosion, active mass particle size, porosity,

KLÍČOVÁ SLOVA

olověná baterie, VRLA, rychlé nabíjení, rychlé nabíjení skokově snižujícím se proudem, cyklová životnost, proudové rozložení, stratifikace elektrolytu, nevratná sulfatace, koroze mřížky, velikost částic aktivní hmoty, porózita.

MÍSTO ULOŽENÍ PRÁCE

oddělení pro vědu a výzkum FEKT VUT v Brně

Table of Contents

Initialization

The present environmental situation and pollution development is considered to be a global problem. The environmental situation in worlds' largest cities is at certain conditions already considered to be harmful for human. There are many ways how to reduce environmental pollution and limit the adverse development. Attention must be given to the transportation industry. Vehicles powered by internal combustion engines (ICE vehicles) are a great source of urban local pollution. Alternative types of vehicle with practically direct zero emissions exist; electric vehicles (EV) powered by batteries have these properties and have been known for the same period as ICE vehicles. Unfortunately good environmental parameters of EV were initially overcome by technical properties of ICE vehicles, later technical-financial-psychological embarrassments were added. The present bussiness situation of car manufacturers and oil industry including existing ICE vehicles infrastructure hinder any change and tendency to introduce EV into the present market. Although the development of EV has been sometimes intensively and sometimes moderately running, the situation remains about the same. A conservative society that doesn't like changes and any reduction in comfort, supported by strong automobile and oil industries offer many reasons against EV introduction. Developed EV parameters reflect higher EV cost. Running development of ICE vehicles seems to be also set to compete EV technology. **The general task of this work may be understood as developing operational EV battery parameters at low EV cost. Particularly this work is concentrated on the thin tubular valve regulated lead acid (VRLA) batteries and degradation processes at the fast charge.**

1 Lead-acid accumulators

Although lead-acid accumulators do not have better parameters in comparison to the other common advanced electrochemical accumulators (NiCd, NiMH, Li-ion) they are still widely used mainly as starting and stationary batteries. The main advantage of the lead-acid accumulator is its low cost. Some of the operational properties are also very welcomed like reliability, higher operational voltage range, low internal resistance, wide experience and deep knowledge about this electrochemical system. Cycle-life capacity decease is usually gradual allowing in time system repair.

The thesis lists the main properties of lead acid accumulator, describes the main designs of the accumulator and individual components.

Special thin tubular valve regulated lead-acid accumulators (VRLA) were developed and produced in single cell and 12V block design by CMP Exide Ltd. company. The tubular plates are convenient for traction applications due to an increased durability at a heavy duty EV operation. The drawback of typical tubular plates is a low power performance and a low charge acceptance. Therefore the thin tubular electrodes were designed and produced for enhanced high rate performance. This thin tubular VRLA accumulator was designed by the latest knowledge with many experience and produced by modern, highly precise technologies in CMP Exide Ltd. company in Great Britain. The accumulator may be described as follows: VRLA accumulator of 70Ah nominal capacity with absorptive glass mat (AGM) separator, consisting of six positive

tubular plates of 3.5mm thickness and seven grid negative electrodes. High Sn content lead-tin-calcium alloy was used for the thin cast spines current collector for enhanced spines corrosion resistance. Spines elliptical cross-section was used for 7% larger surface area in comparison to the equivalent circular cross-section spines. Each positive plate contains 25 parallel connected tubes.

Theoretically at the same active mass utilization the negative electrode is oversized for 8.5% in comparison to the positive electrode. Overall active mass utilization related to the positive active mass is 29%. Parameter γ reflecting the amount of the positive active mass (PAM) related to spines' surface area was about 2.5 times reduced to 0.95 g/cm^2 in comparison to the equivalent conventional tubular positive plate electrode (tube diameter 10mm). In the same manner the spine surface current density was reduced for the rate 4.5C from 6.7mA/mm^2 to 2.8mA/mm^2 for the theoretical homogenous current distribution over the electrode. The active mass momentum parameter was specified in this work for description of current path length through the active mass to the current collector, this parameter is 2.3 times lower at the thin tubular CMP plates in comparison to the conventional tubular plate.

1.1   Methods for lead-acid accumulators analysis

Degradation processes of lead-acid accumulator are listed and described in this thesis. Various analysis were used for identification of dominant degradation processes - examination of individual degradation processes rates that limit the cells' parameters and cycle life. These methods for lead-acid accumulators analysis are described in this work.

1.1.1   The current distribution analysis

The current distribution over the negative electrode plate was analyzed by a new measuring technique developed for this purpose within this thesis. This method is based on voltage measurement over the negative electrode as on shunts. The problem of high variation of these shunts resistance due to great resistance change of charged-discharged active mass is overcome by regular current injection into the electrode for "calibration" of these shunts. This method provides sufficient and reliable results for current analysis over the electrode.

2   Experimental

2.1   Fast and normal charge

Typical **normal charge** regime **I-U-I$_{a1}$-I$_{a1}$** was used in reference experiments within this thesis. The current rate of the initial constant current charge phase was limited to C/5 rate, the constant voltage charge phase is limited by current decrease below C/28. Two final constant current charge phases are performed by C/35 and C/70 current rate, these steps are also voltage and time limited. Typical time duration of normal charge regimes is 4 to 12 hours. The final low rate charge is used for charge rebalance of all cells in series and some overcharge is necessary for complete battery recharge. At VRLA cells it is not easy to optimize the charge process because rate of processes in the cell differs with aging. Briefly explained, at beginning higher gassing rate is attributed to the higher initial electrolyte saturation, while it gets reduced the oxygen recombination efficiency rises. The oxygen starts to evolve at the positive electrode due to the

positive electrode limited capacity and recombine at the negative electrode. When the final charge current is low enough then the oxygen recombination at the negative electrode consumes the charge and depolarizes the electrode. Then the negative electrode can not be fully charged and undercharge degradation starts, Atlung S. et al. **[5]**. When the final current is too high there is high gassing rate leading to the cell the **drying out** process, high rate of oxygen cycle running for a long time may lead to the **thermal runaway**. It was demonstrated that voltage limit of these final constant current steps have great influence on the gassing amount, the limit increase from 2.6V to 2.65V caused three times higher gassing amount. On the other hand this voltage limit increase leads to stabilized discharged capacity that may reflect higher AM recharge at lower charge rate.

The main basic requirements for the **<u>fast charge</u>** is the short charge duration without any abuse to the battery. Some reports claim positive effects of fast charge to the cycle life sometimes in a few folds range that are explained by better charge efficiency, lower overcharge and the AM structural protection, particularly maintaining original fine crystal structure. For the fast charge the battery charge acceptance and internal resistance (IR) compensation is very important. Sometimes pulse charge technique is used, this method was originally invoked by the battery voltage measurement during no-current pauses, so called resistance-free voltage was introduced by Kordesch K.V. et al. **[9]**. Later the resistance-free voltage controlled charger was patented and realized by Nor J.K. et al. **[10]**& **[11]**. The internal resistance compensation is discussed in the thesis, practical realization of charger providing "on-line" IR compensation is a technical problem. It would require very fast and precise measurement and it would reflect in the non-feasible investment costs. For the proper diffusion overpotential compensation a long time measurement would be required, that is not practical at the short time duration fast charge.

When any fast charging is reported there must be always the question: **How does the particular fast charge regime influence the battery cycle life?** There are always requirements for a short charge duration and also for a long cycle life!

The fast charge is a great task of this work consisting of setting and optimization a fast charge procedure to achieve a short charge time duration with minimal abuse to the battery – mainly minimal gassing and temperature rise. The fast charge procedure should not limit the cycle life in comparison with the normal charge. Performed analysis after the end of life on the normal cycled batteries and on the fast cycled batteries should indicate any differences in failure modes that may prove or exclude some of the claimed promising beneficial effects of the fast charge.

Parameters of unknown accumulator for fast charge regime may be determined by the help of U-I-SOC map measurement, such of map was measured and created for the tested VRLA cell in the current range 0.2C – 3C and in the SOC range 0-100%,refer to the picture **Fig. 1**. The bold curve in the map demonstrates charge acceptance curve of the cell.
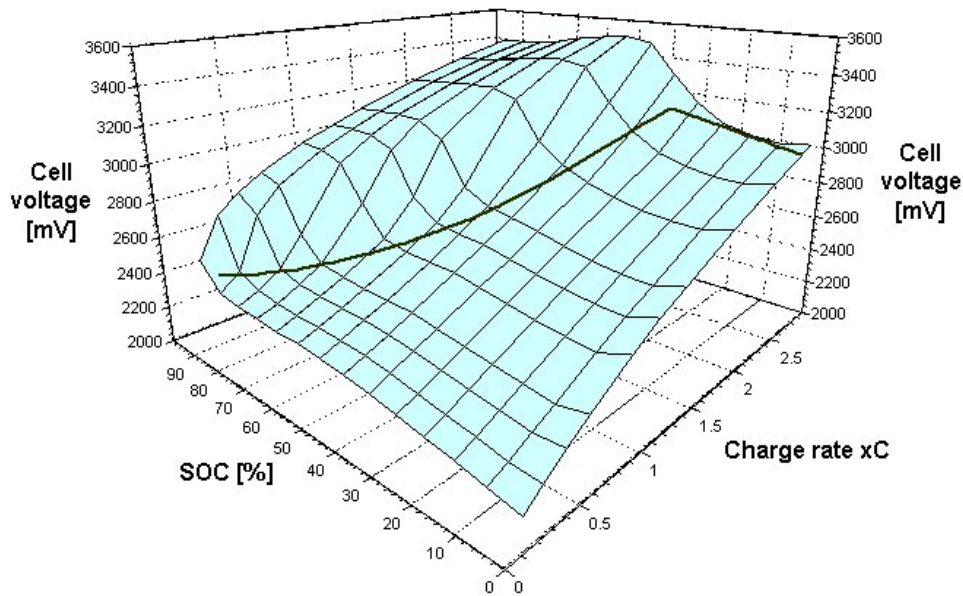
Fig. 1 Cell voltage map U-I-SOC.

Within the project a new **<u>current step down fast charge procedure</u>** was developed, tested and optimized. This unique fast charge regime has defined constant current charging steps with voltage limitations. The superior property of this fast charge regime is the independent definition of currents and voltage limits separately in individual charge steps that belong to a certain SOC range. This feature is very powerful, universal and adaptive to set this fast charge for any battery and charge acceptance. Thus internal resistance (IR) and diffusion overpotential were well empirically compensated. The initial steep cell internal resistance decrease at the beginning of charge at fully discharged battery was introduced to be considered by the charge control mechanism. Battery temperature compensation of these voltage limits is included in the charge control. This temperature compensation effectively protect the battery against steep temperature rise and temperature abuse to the battery. Practical realization of such charging steps was done without serious problems on Digatron charging equipment and Digatron BTS software.

The unique about this current step down fast charge is not a high current of 4C but independent setting of individual current steps and with voltage limits with a respect to these parameters:

- **At the beginning of charge internal resistance rapidly decreases after the full discharge.**
- **Internal resistance empirical compensation.**
- **Diffusion overpotential empirical compensation.**
- **Temperature compensation.**
- **Optimized for minimal gassing.**
- **Proper negative electrode polarization (final pulses).**

While considering all these parameters the voltage limits could be set to higher level, e.g. at the 4C charge rate step the voltage limit was optimized even more then 2.5 V/cell while gassing rate and temperature increase was maintained minimal.

Empirical compensation of the diffusion over-potential was done in order to compensate increased cell potential rising from electrolyte concentration gradient that appears during the higher rate charge. Local concentration of electrolyte in active mass pores during the fast charge increases with a higher rate then diffusion kinetic may overcome. Diffusion overpotential compensation "on-line" is impractical because it is very long lasting measuring process related to the charge duration prolongation. This diffusion overpotential is therefore empirically compensated in these individual charge steps of different charge rates.

Voltage limits are temperature compensated for –4mV/K.cell this provided very effective temperature control mechanism. Battery temperature is an important and necessary parameter to be controlled at a fast charge.

It must be mentioned here that the fast charge doesn't recharge batteries to 100% SOC, usually it recharge batteries to about 90% SOC. The main reason is that the last few per-cents of recharge take very long time as accumulator charge acceptance is decreased.

The negative electrode that is oversized for 8.5% in comparison to the positive electrode. There may appear a serious problem of particularly the negative electrode undercharge at the fast charge. To eliminate this problem a short time pulses were introduced at the end of the fast charge. These relatively low rate current pulses are used for the negative electrode polarizing at reduced gassing. It is proved and demonstrated in this work by the Hg/Hg_2SO_4 reference electrode measurement that during the final fast charge pulses the negative electrode is mainly polarized while no gas emission through the cell valve was measured.

Tests performed on thin positive tubular plates VRLA cells proved a short charge time duration, some results are listed in the table **Tab.1.**

Tab. 1 Duration of the fast and the normal charge at tubular plate VRLA cells.

Charge regime	Duration of the charge process to		
	50% SOC	80% SOC	100% SOC
Fast charge	10 min	22 min	53 min
Normal charge	2.3 h	3.7 h	5h

Actual SOC is based on the previous discharge capacity.

This current step down fast charge regime was finally tuned for the minimal charge time duration, minimal gassing, and minimal temperature rise. Then the charging time duration to 80% of SOC had been prolonged to about 30min.
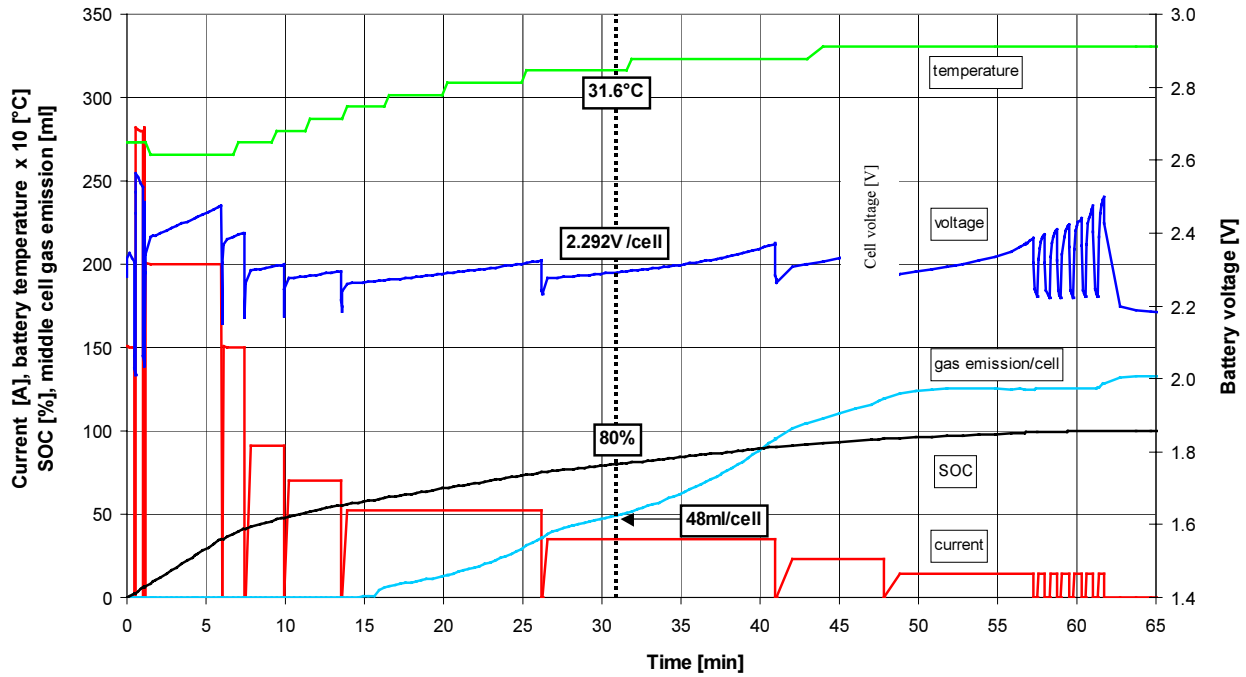
Fig. 2 The current step down fast charge procedure tuned for tested
12V tubular plate VRLA battery.

**THE FINAL OPTIMIZED CURRENT STEP DOWN FAST CHARGE PROCEDURE FOR THE 12V TESTED
BLOCK IS PRESENTED IN THE GRAPH FIG. 2.**

The usual temperature rise at this fast charge was measured for about +7K. No any auxiliary cooler or fan was used for cells, cells were standing on the test bench in an ambient room temperature, in the case of cells connected in series cells were tightly fixed together without any gaps in between cells. In the case of 12V blocks batteries tests were performed in a water basin, water medium was filled up to 2/3 of the block height. The water medium was kept at constant temperature 35°C.

As was mentioned the practical requirement for a short time duration of EV battery recharge may be achieved by fast recharging to about 90% SOC. In a practical application of EV the operational readiness to drive as soon as possible after the discharge may overcome the necessity for the maximal driving range. In that case recharge less then 100% should be allowed. However it is very important to regularly perform full charge:

- Complete recharge prevents irreversible sulfation. Complete AM charge prevents large lead sulfate particles grow. It is demonstrated in this work that the periodic complete recharge is important for fast charged batteries, particularly for protecting bottom parts of electrodes.

- Complete recharge re-balances series connected cells/batteries SOC level by applying the low end of charge current, after the full charge with a certain overcharge each cell get to 100% SOC.

It is important to say that the only fast charge that incompletely recharge batteries would cause serious undercharge problems and fast degradation with early capacity loss. Individual series connected cells have different capacities and therefore some certain amount of overcharge is always necessary to equalize individual cells SOC although it brings gas emission and batteries heat up.

If not otherwise stated, the "fast charge" cycling herein means always this scheme: four consecutive current step down fast charge cycles & one the normal I-U-I_{a1}-I_{a2} charge cycle.

The other aspect of EV operation is the DOD level. In the real operation EV batteries are not usually discharged to 100% DOD, they are discharged only to about 80%. EV battery discharge may be simulated by the standard ECE15L80% Pb dynamic discharge profile, **[6]**. The discharge is limited to 80% DOD or by specified limiting battery parameters (minimal voltage, power).

2.2   Individual voltage scattering and gassing in series connection

Practical measurements at EV operated at the Technical University of Brno indicated more homogeneous individual voltages of 14 blocks 6V 170Ah while the EV battery was fast charged with 0.8C rate in comparison to the 0.08C rate of the normal charge (EV on-board charger).

Therefore an evaluation of individual cells voltages connected in series was done for the higher and lower charge rate. Results are important for consideration of a charge equalization system that should control individual blocks charge in a case of EV by voltage monitoring.

Based on the achieved results it may be concluded that a charge equalizing system seems to be beneficial for normal charged cells series string, it would equalize charge among different capacity cells while reducing overcharge and gassing. At the fast charge a charge equalizing system would be beneficial only at the final stages where the current rate is lower. That reduces power requirement and investment costs of such of system applied at the fast charge.

It was demonstrated that higher charge rate results in more homogenous voltage distribution of individual cells in series. Individual cells voltage difference related to the internal resistance is overcompensated by kinetic over-potential.

The gassing amount of the current step down fast charge is 5 to 10 times lower comparing to the gassing of the normal charge. However the charge return of the fast charge is only ~90% SOC. It is more realistic to compare average gassing of the fast cycling procedure (4x fast charge cycle & 1x normal charge cycle) that results in average 4 times lower gassing of the fast charge.

2.3   Parallel connection of single cells

Test with parallel connected cells was done in order to examine current distribution between parallel connected sub-strings at the normal and at the fast charge. For certain applications proposals for batteries parallel connection appear.

Measured results proved that the parallel connection of cells/batteries is usually associated with different energy throughput in parallel connected sub-strings. The fast charge applied would have a beneficial effect in the faster parallel sub-strings recharge balance.

2.4   Analysis of the current distribution over electrodes' plate area

A homogeneous current distribution over the electrodes' plate area would be beneficial for uniform AM utilization during the charge/discharge reaction, homogeneous degradation and general cycle life parameter. Current distribution over the electrodes was evaluated under higher and lower charge and discharge current. Alternative cell design in the manner of different position of electrode lugs was tested. The standard lead-acid cell design has both the negative and the positive electrodes plates lugs on the top of the cell that is the easiest way for manufacturing, this is called **TOP-TOP (T-T)** design herein. From the current distribution over the electrodes plates area this design is not the ideal, therefore the alternative design was tested here, the positive and the negative electrodes' lugs were placed on the opposite sides of electrodes, this alternative design is called herein **TOP-BOTTOM (T-B)**. It is supposed that such of design has a beneficial effect to the current distribution over the electrodes. Refer to the picture **Fig. 3**.

The new mentioned measuring-analyzing method was invented and realized within this thesis. The method for the current distribution measurement over the electrode plate area including some limitations is described in the work. Briefly it may by explained by the scheme on the picture **Fig. 4**. The method principal is based on the voltage measurement "*M*" on a variable shunt (-electrode), the shunt variation problem is solved by regular constant current injection "*I*" (like re-calibration) that creates potential map on the shunt (- electrode) equal to the homogeneous current distribution. Final results are done by comparison of the created potential map and the actual voltage measurement.
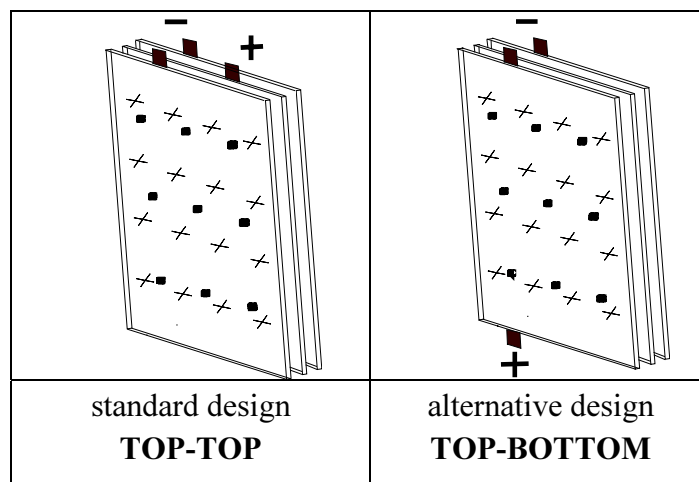

| standard design **TOP-TOP** | alternative design **TOP-BOTTOM** |

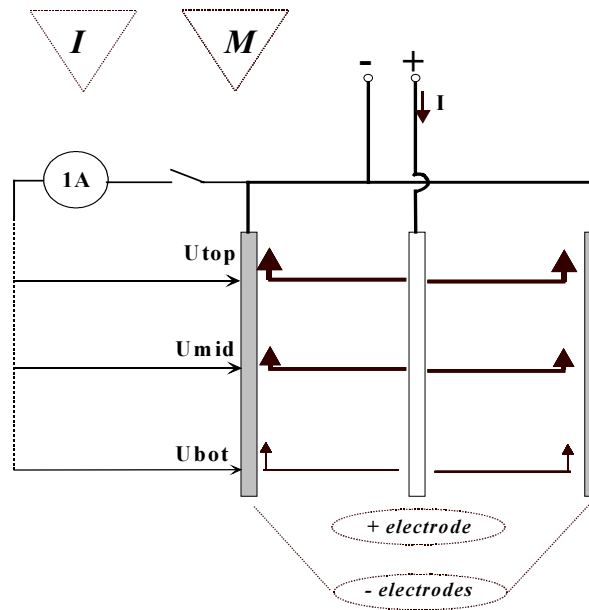**Fig. 3** Orientation of electrodes and electrodes' lugs.

Fig. 4 Schematic explanation of the current distribution measuring method.

2.4.1   Results of the current distribution over the electrodes' plate area

When the current distribution over the electrodes' plate area is uniform with the simulated homogeneous current distribution then the ratio value in this analysis is 0.5 or 50% respectively. In the thesis results of this analysis are demonstrated by the means of colored surface graphs. These results are shortly described here in tables **Tab. 2** and **Tab. 3.**

Tab. 2 Evaluation summary results of the current distribution at discharge

Evaluation summary at DISCHARGE	
DOD level	Discharge at a lower DOD level (beginning of discharge) is closer to the homogeneous discharge in comparison with higher DOD levels.
Current rate	Discharge at the lower current rate is slightly closer to the homogeneous current distribution in comparison with the higher rate. Discharge current rate influence is very limited!
Cell design	Discharge of the cell with the alternative design (**T-B**) has significantly better current distribution in comparison with the common cell design (**T-T**).

Tab. 3 Evaluation summary results of the current distribution at charge.

Evaluation summary at CHARGE	
SOC level	The initial worse current distribution at about 20% SOC gets more homogeneous at about 50%SOC, at the fast charge smaller value remains at the right bottom corner. At about 75% SOC the distribution turns worse again at the bottom part and particularly at the bottom corners. At 90% SOC the surface current density at the top and at the mid

	part starts to decrease and the bottom part starts to rise. At 100% SOC the top and the middle part is decreased while the bottom part risen.
Current rate	At the (**T-T)** cell configuration in any case higher charge current rate pushes the bottom part surface current density down. At the (**T-B)** cell configuration the current distribution is less sensitive to the rate.
Cell design	The alternative (**T-B**) configuration seems to be beneficial at the higher current charge. Then the distribution in the top-bottom direction is more equalized but differences appear at left-right direction that may be a result of non-symmetric lugs placement.

This is an important fact for **the fast charged battery that is recharged to approximately 90% SOC, the bottom parts of electrodes are NOT fully recharged**.

The reason for the better current distribution on the electrode plate under the lower charge current may be explained by different cell resistance at different current rates – dynamic resistance. When the only ohmic linear resistance would be considered, at the higher current rate higher absolute current differences between the top and the bottom part would be achieved, the relative (current equalized) differences would be the same. The cell resistance is however lower at the higher current rate. The lower resistance at higher current is based on lower charge transfer resistance. It may be explained by the dependence of the current on the charge-transfer overpotential example that is presented on the picture **Fig. 5**. This dependence example is calculated by Butler-Volmer equation, Regner A. et al. **[12]**, Bard A. et al. **[13]**:

$$i = i_o * \left[\exp\left(\frac{\alpha * F}{R * T} * \eta \right) - \exp\left(-\frac{(1-\alpha) * F}{R * T} * \eta \right) \right]$$

In this equation $\underline{\alpha}$ and $\underline{i_o}$ are kinetic coefficients, when (α=0.5) then the curve is symmetric by axes. The example demonstrates lower differential resistance R_2 at higher current rate.
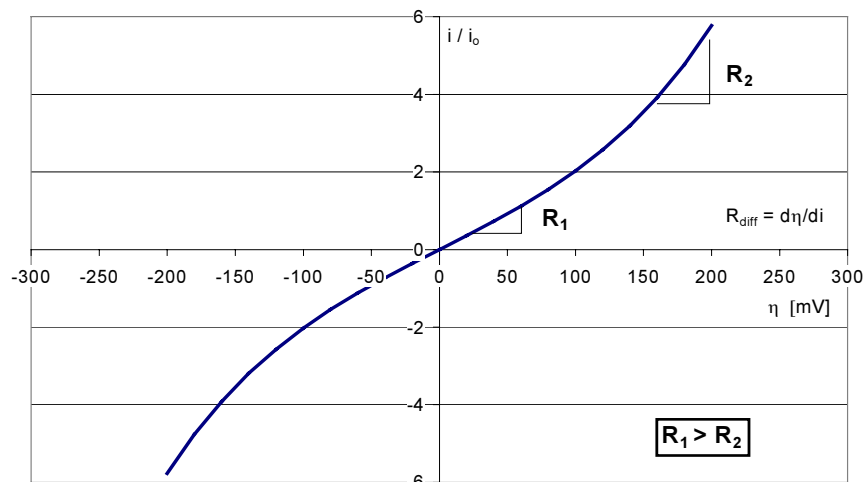

Fig. 5 Butler-Volmer equation - dependence of the current on the charge transfer overpotential.

When there is the highest surface current density at the electrodes' top part, the resistance of this part is lower in comparison with the bottom part, this forces even higher current at the top and causes the adverse current distribution effect under the higher current rate. This is a system with the positive feedback, high current is attributed to lower resistance and that forces higher current.

<u>2.4.2</u>   <u>Analysis of the current distribution at individual electrodes' plate</u>

Analysis of the current distribution at individual electrodes' plates was also done at lower (C/5) and higher (1C) charge and discharge current. Currents of individual negative plates were measured.

While comparing current distributions among individual negative electrodes' plates at the higher (1C rate) and the lower (C/5) current rate for particular SOC/DOD levels there are not significant differences. The side negative electrodes have about a half or higher current in comparison to the other negative plates. The side negative electrode plate has only one counter positive electrode plate. Theoretically these side plates could be down-sized concerning active mass however this would bring additional cost to the final product.

Results of this measurement can not be fully compared with parallel connected cells. In the case of parallel connected electrodes' plates there is a conductive bridge though the separator saturated with electrolyte at these plates sides. This equalize differences among those electrodes' plates. This mechanism does not work in the same magnitude for the top-bottom current distribution over the electrodes' plate area. The conductive bridge between two different potential places is much longer (top – bottom of the plate) in comparison to the plate – plate current distribution where the inter-plates electrolyte bride is in the same height of those plates just crossing-over the thin negative plate in between.

Conclusion of the current distribution measurement

The method of potential distribution measurement over the negative electrodes' plate area may be used for the current distribution analysis inside the cell when accompanied by additional measurement (current injections). Current injections method is a good way to find the homogeneous current distribution model over the electrodes' plate area at the particular SOC-DOD with a sufficient precision.

Summary of the current distribution over the negative electrodes' plate:

- **Higher charge current rate is attributed with worse current distribution, higher charge current forces lower currents at the electrodes' bottom part.**
- **At the charge process the higher current rate adverse effect to the current distribution is stronger in comparison with this effect at the discharge process.**
- **Complete recharge of the bottom part of electrodes proceeds close to the 100% charge return. The fast charged cell may particularly suffer from electrodes bottom parts undercharge.**
- **Particularly at discharge the alternative cell design so called TOP-BOTTOM having alternating electrodes lugs placement on the top and on the bottom has significantly better current distribution in comparison with the standard TOP-TOP lugs configuration cell. At charge this positive effect was indicated in lower extent.**

Current distribution among individual electrode plates in one cell is minimally effected by the current rate .

2.5   Cycle life tests

Cycle life tests were done on single cells, series connected cells string and series connected blocks. There were practical reasons to do so, at first general parameters of new single cells prototypes were examined including individual electrodes behavior. The current step down fast cycling was initially tested and tuned also on the single cells. Single cells were tested in series and parallel connection in order to check uniformity and individual cells behavior in a string operation. The fast charge optimized and tuned for single cells was tested on single cells series to identify any problems and optimized the fast charge regime for series operation.

The 12V blocks as uniform modules for any further practical application were also tested. Behavior of individual blocks was examined in five series connected blocks string. The fast charge was finally tuned for these 12V blocks and used for the five block string cycling.

2.5.1   Cycle life test procedures

Cycle life of single cells and series connected cells was done by the normal and the fast charge and C/2 constant current discharge down to 1.7V/cell. Cycle life tests were done also on series connected blocks. Both charge regimes: the normal and the current step down fast charge were tested however discharge was realized by the mentioned dynamic ECE15L80%Pb discharge procedure, refer to **[6]**.

2.5.2   Cycle life results

Cycle life results of series connected single cells cycling are presented on the picture **Fig. 6**. Both short strings of single cells had 6 cells in series. In order to evaluate maximal cycle life of these developed cells, it was allowed to exclude the weakest cell from the string. When any particular weak cell limiting the string capacity was detected then it was removed from the series without replacing it. Numbers of remaining cells in these strings are shown in the graph **Fig. 6**.

At the normal cycled string discharge capacity decline was measured during the first 20 cycles although voltage limit of two final constant current charge steps was increased at cycle nr. 9 from 2.6V/cell to 2.7V/cell. Following capacity recovery returned the discharge capacity to the nominal value. Then the discharge capacity started to continuously decrease in the cycle number range 50 to 255. At cycle 78 the voltage limit of two final constant current charge steps was decreased from 2.7V/cell to 2.65V/cell in order to reduce gassing. Capacity increase and stabilization was measured at cycles 240-360 and it may be related to the increased ambient temperature (summer time & limitations of the lab air-conditioning system). The higher ambient temperature caused also increased charge factor. Battery temperature control system was not used at this test. After cycle 380 continuous decrease of discharge capacity was measured. The capacity decrease was stopped at cycle 491 by three weakest cells removal. These three weakest cells caused also high charge factor that was reduced after these cells removal. The best normal cycled cell achieved 670 cycles.
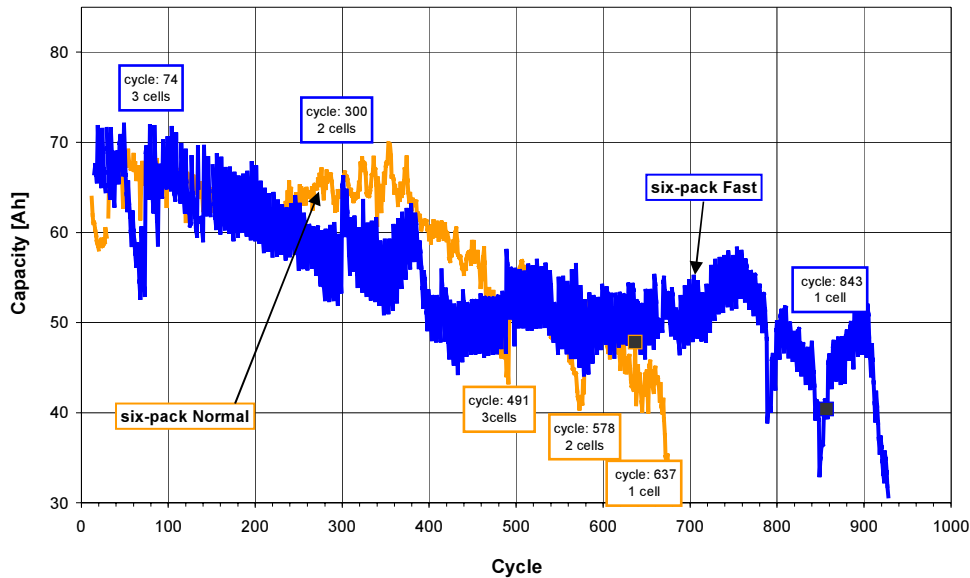
Fig. 6 Short series string discharge capacity development vs cycle number.

At the fast cycled string there are again the mentioned discharge capacity oscillations. At cycle 50-70 very steep discharge capacity decrease was measured, the decrease was indicated to be caused by three weak cells that were removed from the string at cycle 74 and the discharge capacity returned to the original value. Following capacity decrease in the cycle range 100 to 300 cycle was of about the same extent as the normal cycled string. Cycling of both strings were not synchronized in time and that is why the ambient temperature increase is not seen at the fast charge capacity profile. At cycle 300 cycling was interrupted for 2 month due to a technical problem of the charger. No reason was found for the step capacity decrease at cycles 380-400. At cycles 400 – 780 almost stable capacity profile was measured. The peak capacity drop at cycle ~780 was caused by a weak time interruption of the cycling. The strongest cell achieved 930 cycles.

It may be concluded:
- Not clearly explained capacity decrease and following recovery during the initial 50 cycles at the normal cycled string.
- The initial capacity decrease was not clearly observed at the fast cycled string.
- Oscillations of discharged capacities at the fast cycled string were caused by the fast charge sequence: 4x fast charge cycle & 1x normal charge cycle. The fast charge recharge these cells for about 90% SOC and the normal charge must equalize the missing charge.
- Some recovery of the discharge capacity belongs to the removal of weaker cells.
- Some swings in discharge capacity were caused by the ambient temperature change in the test laboratory related to summer-winter time. These cells were cycled without any special temperature control system.
- The best cell cycle life of the normal cycled string was about 670 cycles and of the fast cycled string it was about 930 cycles. The fast charged string achieved about 40% longer cycle life comparing to the normal charged string.

Charge factor represents Ah charge ratio between Ah charged and Ah discharged in one cycle. Charge factor at the **normal charged string** alternates around **113%** while at the **fast charged string** the **average value of the charge factor** (4 fast charges cycles and 1 normal charge cycle) alternates around **103%.** The lower average charge factor at the fast charged string reduces gassing and cell drying out risk. It also brings a better coulombic efficiency.

Cycle life results at series connected blocks with dynamic ECE15 discharge Two normal cycled strings are marked **string A** and **string B**, the **string B** had increased specific electrolyte gravity (from $1.3 g/cm^3$ to $1.32 g/cm^3$) in comparison to these other strings and single cells. The fast charged string is marked **string F**. Cycling of these series connected blocks was done in temperature controlled water bath of 35°C, the water level was adjusted to ¾ of the blocks height. After the pre-cycling and initial blocks characterization, 80% of the ECE15LPb dynamic discharge had to be determined for the cycle life tests. A few cycles always with the normal charge and the ECE15LPb discharge were performed. For all these strings 80% of the initial ECE15LPb dynamic discharge was set to 54Ah (average of three ECE15LPb tests at each string), this value should be also the limiting parameter for cycle life determination.
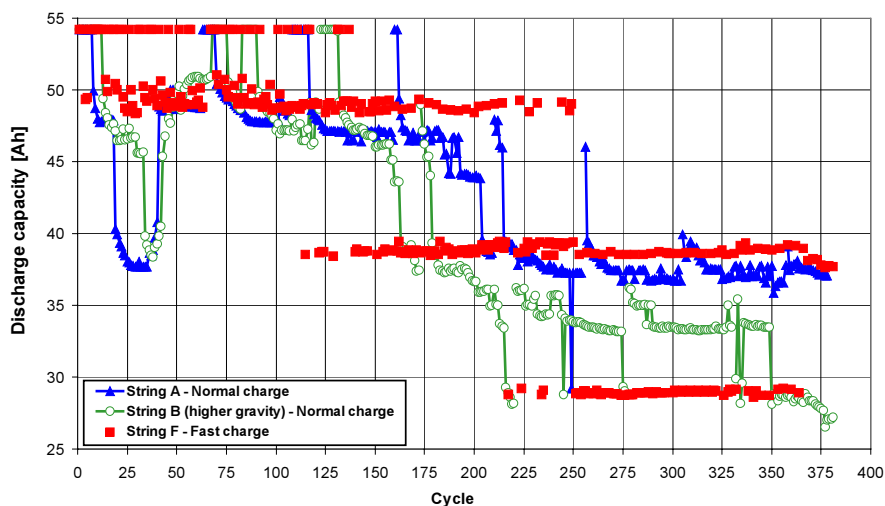

Fig. 7 Cycle life tests: series of 12V blocks, fast & normal charge, ECE 15L Pb 80% discharge.

The cycle life development of the dynamic discharge ECE15L80%Pb capacity is presented in the graph **Fig. 7**. Note that the maximal discharge capacity is limited by 80% that is 54Ah limited discharge. Very clear steps of the discharge capacity development were caused by the ECE power discharge requirement in one step of the suburban part. When this step was overcome then the following urban part was usually passed too. Cycling of these strings was stopped in equivalent cycle number to perform postmortem analysis under the same battery conditions. Although the cycling was stopped after about equal number of 380 ECE cycles difference in the strings performance is indicated by ECE discharge capacities and also by the C/5 discharge tests that were regularly done during the cycling, refer to the **Fig. 8**. The ECE discharge capacity was slightly higher at the fast cycled **string F** and the lowest at the normal cycled **string B** with higher gravity electrolyte, C/5 discharge capacities had the same order and was even better at the **string F**.

- The initial capacity drop within 50 cycles at the normal charged blocks series **string A & B** was clearly observed, the same observation as at cells in series cycling at the normal charged series. **No any significant initial discharge capacity drop was observed at the fast charged blocks series.** We do not have any clear explanation why the initial discharge capacity drop appears and how it is itself recovered.
- The step decrease course of the discharge capacity is caused by the ECE dynamic discharge, when batteries pass the suburban part then they usually overcome the subsequent four urban parts of the discharge.
- After the parameter checkup always a short time capacity recovery was observed.
- At the **fast charged string F** (full squares) there are discharge capacity oscillations due to the cycling sequence 4x fast charge cycle & 1x normal charge cycle.
- The **fast charge string F** had the best cycle life performance. The **normal cycled string B** (higher electrolyte gravity) had the worst cycle life performance. While the **normal cycled string A** performance was in between strings **F** and **B**.
- Series connected blocks at the **string B with the higher specific electrolyte gravity** that was normal charged did not demonstrated enhanced performance at ECE15L80%Pb cycling in comparison with the normal cycled string A with lower gravity electrolyte.

The graph on the picture **Fig. 8** indicates that the C/5 rate discharge capacity of the fast cycled **string F** is stable throughout the cycle life in comparison the to the ECE discharge. While the discharge capacity decrease of the **string A & B** seems to be of the same slope for both C/5 and ECE discharge, the slope of the **string F** C/5 capacity decrease is lower.
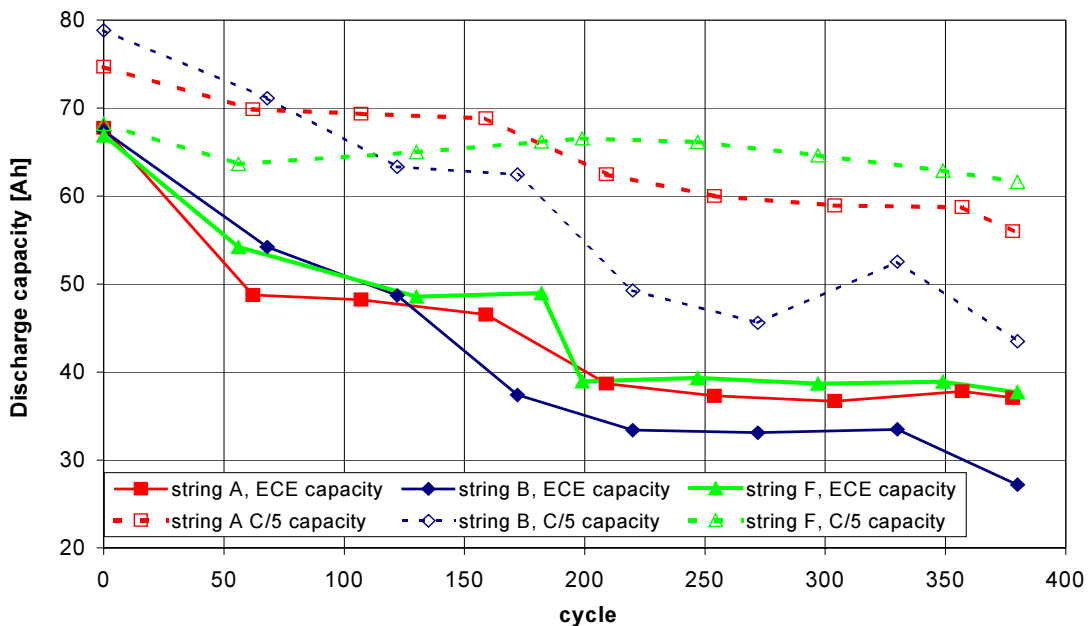

Fig. 8 Discharge capacity results of regular parameters C/5 discharge checkups and ECE discharge.

The fast cycled string F has stabilized low rate discharge capacity throughout the cycle life while dynamic ECE15LPb (high rate steps) discharge capacity dropped.

ACHIEVED CYCLE NUMBERS OF ALL CYCLE LIFE TESTS ARE SUMMARIZED IN THE TABLE TAB. 4.

Tab. 4 Summarized results of cycle life tests

Connection	Charge	Discharge	Cycle life / Remaining cap.*
Single cells	Normal	C/2 cut-off 1.7V/cell	340/38Ah
	Fast	C/2 cut-off 1.7V/cell	340/45Ah
Series connected cells	Normal	C/2 cut-off 1.7V/cell	670/40Ah
	Fast	C/2 cut-off 1.7V/cell	930/40Ah
Series connected blocks	Normal	ECE15	436/44Ah
	Fast	ECE15	469/62Ah

* Remaining capacity of blocks series is expressed for
C/5 discharge to 1.7V/cell.

Conclusion about the cycle life may be done here on the basis of three independent types of tests (single cells, series connected short cells string & blocks strings cycling). The fast charge was beneficial in all these tests that may be expressed by these statements:

- **At the end of cycling at the same cycle number the fast cycled cells had higher remaining capacities.**
- **For the same end of life discharge capacity limit the fast cycled cells achieved higher cycle number.**

Charge acceptance development

The development of the charge time to different SOC related to the previous discharge during the fast charge procedure was evaluated. Within the first 100 cycles an increase in required charge time to specified SOC levels was observed. Surprisingly in the following the charge time to the different values of SOC was reduced and this is not only caused by the decrease in capacity. So it is noted that the speed of charge acceptance is enhanced at higher number of cycles.

Conclusion about the cycle life

➢ *Single cells cycling: Cycle life of single cycled cells was relatively poor of about 340 cycles however it must be said that this cycling was done in order to optimized and tune both charge procedures. Charge factor was low and it is supposed to cause undercharge effects.*

➢ *Cells short series string cycling: Two packs of six cells in series connection were normal charge and fast charge cycled. Cycle life results of the fast charged series was about 40% longer in comparison with the normal charged series, achieving 930 and 670 cycles respectively. These cycle life results belongs always to the strongest cell in six cells series.*

➢ *Series connected blocks: Five blocks in series were connected in each string and these strings were cycled by ECE15LPb80% dynamic discharge cycle life procedure while normal and fast charged. Achieved cycle number was lower comparing to series connected cells, 469 and 436 total cycles for the fast and the normal charge respectively.*

➢ *The fast charge procedure seems to be beneficial for the cycle life however the realistic cycle life prolongation effect can be expected here rather in the range of 10-20% than of 40% as was achieved at the short string cells series cycling.*

➢ **_Efficiency: It was demonstrated that the fast charge has higher coulombic efficiency. Due to lower average charge factor the overcharge (cells gassing & all those secondary reactions) may be reduced. It lowers drying out risk._**

➢ **_Enhanced charge acceptance was measured at the fast charge at higher cycle number._**

2.6 After cycling analysis – Electrical tests

Electrical tests after the end of life were done as the initial part of the postmortem analysis. The discharge capacity distribution at series connected blocks and at individual cells was analyzed at electrical tests. The capacity distribution indicated the weakest cells in those block. Electrical tests with reference electrode indicated the electrode that limited the cell performance.

2.6.1 End of discharge blocks voltages

The end of C/5 discharge blocks voltages at all three strings were monitored after the normal charge. In this test each string were discharged with C/5 current down to average 10.2V per block, that mans that the string cut-off voltage was controlled by the voltage limit set by the number of blocks multiplied by 10.2 V. Block with the lowest end of discharge voltage is the weakest in the string. Results demonstrate that the fast charged **string F** had the most uniform end of discharge blocks voltages. The highest end of discharge voltage spread was measured at the normal charged **string B**. It must be taken into account that the fast charged **string F** has only three blocks in series in comparison with four blocks in each string **A & B**.

The weakest blocks from the **string A** and **B** were sent to CMP Exide Ltd. (battery manufacturer), analysis at ZSW were done on the strongest and the second weakest blocks of these strings. At the **string F** there were only three blocks in series at the end of cycling, no any significant differences among these blocks were found during the normal charge and the C/5 discharge cycle.

At single blocks capacity distribution among individual cells was examined and results may be comment as follows:
- Discharge capacities by C/5 discharge current were measured for those tested blocks: M31(string F) 70Ah, M26(string A) 65Ah, MB49(string B) 52Ah.
- Blocks MB49 and M31 from **<u>string B</u>** and **<u>F</u>** had one cell of the block significantly weaker then the others.
- The weakest cells were cells nr. 4 from the blocks center and the strongest cells were cells nr. 1 & 6 from the block sides.
- When the weakest cell is excluded than the highest cells' end of discharge voltages uniformity was observed at the block M31 of the **<u>string F</u>**. The worst state was observed at the block MB49 of the **<u>string B</u>**.

In the following analysis the limiting electrodes in these cells were indicated by means of the Hg/Hg_2SO_4 reference electrode. Limiting electrode summary is presented in the table **Tab. 5**.

Tab. 5 Summarized results about limiting electrode investigation.

Test	Charge type	Number of cycles	Limiting electrode
Single cell	Normal charge	340	Positive
	Fast charge	340	Positive
Cells in series	Normal charge	670	Negative
	Fast charge	930	Negative
Blocks in series	Normal charge	436	Positive
	Normal charge (HG)	437	Positive
	Fast charge	469	Positive

Limiting electrode seems to be related to the cycle number. The cell is designed with oversized negative electrode so the positive electrode must be initially and after a low cycle number the limiting one. If the negative electrode is faster aged during cycling in comparison with the positive electrode then the negative electrode may be the liming one.

➢ **At the end of the cycle life <u>individual blocks performance</u> within those strings A, B & F were found the be the most homogeneous at the fast cycled string F.**

➢ **At the end of cycle life the block from the fast cycled series string F had the <u>highest</u> C/5 rate <u>discharge capacity</u>.**

➢ **After the cycling <u>capacity scattering at individual cells within these blocks</u> indicated always the <u>weaker cell</u> nr. 4 that is the cell <u>in the center of the block</u>, while cells nr. 1 & 6 those in the block side position expressed the highest capacity.**

➢ **The highest <u>homogeneous end of discharge voltages</u> were measured at the block from the fast cycled string F.**

➢ **At single cells cycling the <u>positive electrodes</u> were always measured to be the <u>limiting</u>. The <u>negative electrodes</u> were <u>limiting</u> at both short strings series connected cells cycling at higher cycle number.**

➢ **At blocks series cycling the <u>positive electrodes were found to be limiting</u>, however the best state of the positive electrodes was indicated at the fast cycled blocks.**

2.7 After cycling analysis – Cells opening

The blocks weight evaluation indicating cells water loss due to the gassing clearly proved <u>lower water loss = lower gassing at the fast cycled string</u> F. The normal charged string had 1.8 times higher mass loss in comparison to the fast cycled string.

During those <u>cells opening</u> from the short cells series strings, higher separator saturation of the fast cycled string could be observed. Positive plate of the normal charged string was mechanically softer. No any external or obvious internal failure was found at blocks examination during the blocks opening. Higher positive plates expansion degree was observed at block of the normal cycled string A.

2.8   After cycling analysis - Chemical analysis

At the single cycled cells generally higher irreversible sulfation was found and it correspond well to the lower reported charge factor.

Higher electrolyte stratification was analyzed at the fast cycled cells that may be a result of the higher charge rate causing a higher electrolyte gravity diffusing out of electrodes and then more intensive flow downwards (heavier electrolyte) at the same time the current distribution is superimposed to the acid stratification process. The higher sulfation on the bottom of electrodes reduces the electrolyte concentration and the process may continue. The bottom part higher electrolyte concentration also increases sulfation process.

PAM softening and higher drying out was observed at the normal cycled cells.

The fast cycled cells have higher irreversible sulfation particularly on the bottom due to the undercharge and the worse current distribution over electrodes' plates.

At the fast charged battery the AM utilization indicated that there is the capacity limitation by irreversible sulfation at the lower discharge rate. At the higher discharge rate by the dynamic ECE procedure the discharge capacity may be limited by the reduced diffusion kinetic of sulfuric ions into the bulk AM due to the sulfation and acid stratification.

After the end of cycling the fast charge is associated with higher remaining capacity, the positive electrode irreversible sulfation is however the same or higher in comparison to the normal charge. The discharge capacity is limited by the positive electrode and except the irreversible sulfation there is another degradation process at the positive electrode.

2.9   After cycling analysis - Physical analysis

2.9.1   Light microscope analysis, spines corrosion

Significantly higher corrosion of the positive electrodes' spines - current collector was analyzed for the normal charged battery, refer to the **Fig. 9**. The corrosion rate is governed here mostly by the positive electrode polarization.
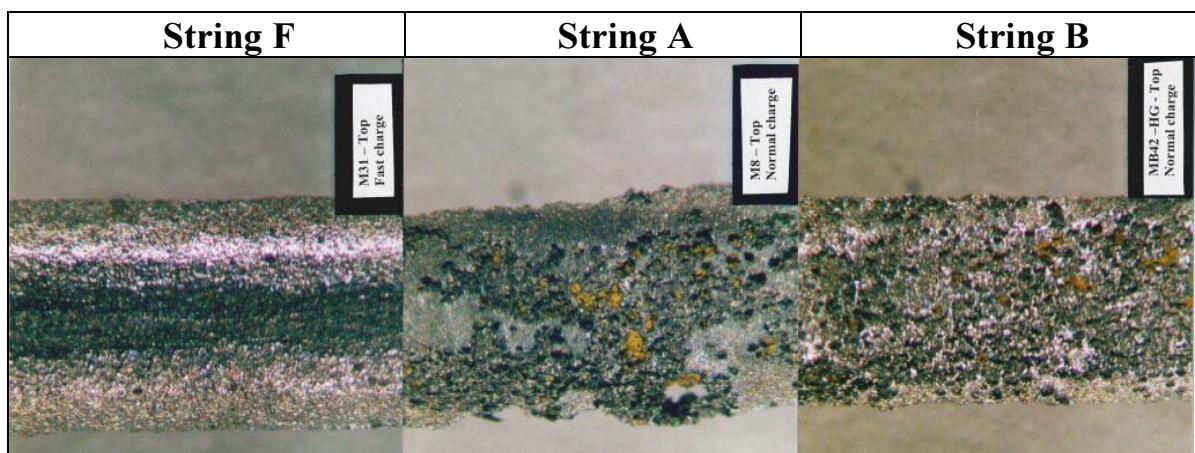
String F	String A	String B

Fig. 9 Photos of light microscope of spine's surfaces from
the top central electrodes' part.

Corrosion dependence on the potential was measured by Lander J. et al.[7]. High corrosion peak is measured at the positive electrode potential around 0.9V against Hg/Hg_2SO_4 reference electrode, while at higher polarization the corrosion rate decreases and then starts to rise again at around potential 1.3V.

Consideration of the positive electrode **polarization at different charge regimes** must be done. While the fast charge utilizes higher current higher polarization is expected however the very high polarization is limited to very short time and generally the charge take much shorter time in comparison to the normal charge. A correct comparison of the positive electrode polarization at both charge regime may be realized by histogram of different polarization and stand-in time duration at this polarized state. During the fast charge polarization of the positive electrode is higher that would lead to a higher corrosion however this polarization is limited by a short time duration. The **stay-duration in higher polarization is worse for the normal charge and it forces higher corrosion.**

2.9.2   Scanning electron microscopy analysis

From SEM images it may be concluded that particles at the positive electrode of the fast charged **string F** appears to be slightly smaller in comparison with the normal charged **string A**. These smaller particles may be associated with higher charge current. At the negative electrode of the **string F** there are significant differences between the top and the bottom part, large crystals at the bottom part correlates to the measured high irreversible sulfation. Smaller PAM crystals in a lead-acid battery when charged with higher current were aslo reported e.g. by Ekdunge P. et al. **[8]**.

2.9.3   Flow Particle Image Analysis (FPIA) -PAM particles size & shape

Tab. 6 Results of PAM Flow Particle Image Analysis

	String F – Fast charge		String A – Normal charge	
	Mean particle diameter [μm]	Mean circularity	Mean particle diameter [μm]	Mean circularity
Top	**2.21**	**0.960**	**2.79**	**0.936**
Bottom	**2.71**	**0.956**	**2.63**	**0.938**
Difference bottom to top	+22.6%	-0.4%	-5.7%	+0.2%

This FPIA measurement results in the table **Tab. 6** indicate **significantly smaller particle size at the top part of the positive electrode of the fast cycled cell in comparison to the normal cycled cell**. There are 23% larger particles on the bottom in comparison to the top part of the fast cycled cell. The bottom particles are larger and this is fully in accordance with the current distribution analysis, acid stratification and with the irreversible sulfation chemical analysis results indicting much higher sulfate content at the bottom part of the fast charged **string F**.

This is in agreement with the expectation that higher charge current supports grow of smaller crystals. The effect is based on basic crystallization theories, Erdey-Gruz & Volmer explanation used by Regner A. et al. **[12]**. A crystal may rise from a seed of crystal that must have at least critical size. Higher cathode overpotential decreases critical size of these crystal seeds and there is higher number of the crystal seeds rise. Thus finer crystal structure at higher current charge is maintained while at the normal charge recrystallization cases rise of larger crystals.

2.9.4 Porosity analysis

Porosity analysis was done by two methods, by mercury porosimetry method and by water saturation weight method. Both methods are not ideal and are associated with a system failures when applied for lead-dioxide positive electrode.

PAM analysis by mercury porosimetry

Total porosity results measured by the mercury porosimetry indicate the **lowest porosity at the new cell and at the fast charged blocks of the string F while the porosity of the normal charged blocks of the string A was increased at the end of cycling.**

➢ The positive electrode porosity increases at cycling. Lower porosity increase was observed for the fast charged string F.

➢ The negative electrode porosity decreases at cycling. Significant porosity decrease was observed at the negative electrode of the normal charged string A.

2.9.5 Physical analysis conclusions

➢ **Significantly lower positive electrode spines corrosion was found at the fast charged cells.** It was demonstrated that at the fast charge there is higher positive electrode polarization that is however short in time and overall it reduces spines corrosion.

➢ At both the positive and the negative electrode smaller crystals were observed for the fast charged cells on the SEM pictures. At the bottom part of the negative electrode there were significantly larger crystals of irreversible sulfated $PbSO_4$.

➢ By the laser scattering analysis higher PAM agglomerates compactness & stiffness was measured at the fast charged cells in comparison to the normal cycled cell.

➢ The FPIA measurement results indicated a smaller particles at the PAM sample from the top part of the fast cycled cells.

➢ **Positive electrode porosity increases at the specified cycling. A lower porosity increase was observed at the fast charged cells. Negative electrode porosity decreases at the specified cycling and particularly significant porosity decrease was observed at the normal charged negative electrode.**

2.10   Failure mode at the fast and at the normal charged batteries

The task of this chapter is to summarize all these analysis into a final statement about the VRLA batteries' failure mode at normal and at fast cycling.

Results of individual measurements and analysis are summarized to highlight overall image of degradation processes and their different rates at different charge regimes, refer to the table **Tab. 7.**

Tab. 7 Summarized analysis observation at the end of life of the fast and the normal charge cycling.

Parameter	Fast charge		Normal charge	
	Top	Bottom	Top	Bottom
Positive electrode				
Potential at charge / discharge	↑↑	↑↑	↓	↓
Corrosion	↓	↓	↑	↑↑
Sulfation	↑	↑↑	↓↓	↓
AM utilization	O (original – capacity limited by sulfation)		↓	
Particle size deviation (enlargement)	↓↓	↑↑	↑↑	↑
Porosity change to original	↑		↑↑	
PAM expansion	↓		↑	
Negative electrode				
Potential at charge / discharge	O	O	O	O
Sulfation	↓	↑↑	↓↓	↑
AM utilization	O (original – capacity limited by sulfation)		↓	
Porosity change to original	↓		↓↓	

Legend: ↑↑ very high ↑ high ↓ low O no change   ↓↓ very low
The positive property-influence is marked in this way.

The fast charge:

The fast charge causes higher irreversible sulfation due to the fast charge limited recharge. Higher charge rates lower the current density at the bottom part of electrodes and the undercharge effect is even higher there. The higher electrolyte stratification that is forced by the higher charge rate together with higher sulfation on the bottom cause poor battery performance at higher discharge rates. On the other hand gassing is about four times lower to the normal cycled cells and the drying out risk is reduced as well as the cell swelling. Smaller particle size and AM structure is preserved due to higher charge rates. Corrosion of the positive electrode is significantly reduced due to the fast cycling polarization properties.

Overall results in the table **Tab. 7** indicate that the **positive electrode** is preserved in many parameters at the fast charge however the discharge capacity is limited by the higher irreversible sulfation process particularly at the bottom part probably due to insufficient recharge and the worse current distribution. The positive electrode limits the cycle life at lower cycle number.

The **negative electrode** suffers at the beginning from higher sulfation, capacities of both electrodes get equalized. At the higher cycle number the negative electrode degradation rate may overcome the positive electrode as was indicated at the series connected cells cycling at cycle number of 930 cycles.

The normal charge:
At the normal charge there is a lower irreversible sulfation due to the full charge and a certain overcharge in every cycle. The negative electrode is maintained at good health until a high cycle number.

Sulfation of the **positive electrode** is low. The corrosion is high due to the long stand-in time duration at the normal charge polarization is longer, however the polarization is lower in comparison to the fast charge.

The **negative electrode** is well protected by the full charge and a certain overcharge in every cycle, however at higher cycle number (670 cycles at the cells in series) the negative electrode degradation effect may become dominant and limiting. The negative electrode porosity decreased in higher extent at the normal charge.

The dominant degradation processes evaluated in one sentence: **The fast cycled cells dominantly suffer from irreversible sulfation, lower current density at the electrode bottom part and the electrolyte stratification while the normal cycled cells dominantly suffer from the positive electrode current collector corrosion and PAM softening.**

2.11   SUMMARY & CONCLUSION

The initialization of this work was based on pollution problems particularly in large urban areas. Electric vehicles powered by batteries may significantly improve the present situation. General EV introduction is unfortunately blocked by complex of technical-economical-psychological drawbacks. Batteries are the most critical part in EV, they have very limited parameters and they mainly contribute to EV high investment costs.

This work is focused on a special thin tubular positive plates VRLA batteries with AGM separators that were developed and produced by CMP Exide Ltd. company in Great Britain. VRLA batteries are maintenance free. Tubular electrode plates are suitable for EV batteries due to enhanced durability at heavy duty traction operation. Tubular electrodes have the drawback of reduced power performance and limited charge acceptance. This disadvantage was successfully overcome by the thin tubular plates design. Electrodes with reduced tubes' diameter allow more tubes per a plate and more plates in the cell, resulting in lower current density per a plate and per a tube an in lower cell internal resistance. The current collector is created by spines that were designed and produced with elliptical cross-section, thus spines have extended spines' surface area

and decreased spines' surface current density. Such enhanced tubular plates provide adequate power capability and adequate charge acceptance for EV applications. This design well combines the robust design of tubular plates and good performance of thin plates. The latest knowledge together with many experience were spent on this VRLA battery design including modern and very precise manufacturing. Moreover these batteries should be significantly cheaper in comparison with other advanced traction batteries (NiCd, NiMH or Li-ion). Experiments within this work were done on these new developed thin tubular VRLA batteries.

Limited parameters of EV batteries result in relative short driving range, this drawback may be practically compensated by very fast recharge, therefore fast charging is considered to be very important for EV introduction. Original current step down fast charge method was developed, tested, optimized and finally tuned. This fast charge is a superior charging process that enables independent setting of current and control voltage limits in individual constant current charge steps. This is a unique, powerful, universal and adaptive feature that enables fine fitting and tuning of desired charge regime on particular battery. Individual current steps correspond to certain SOC range. Internal resistance and diffusion overpotential were empirically compensated. The battery temperature compensation was introduced in the charge control system and that makes very effective precaution against thermal runaway and temperature abuse to the battery. The current step down fast charge was optimized and tuned for minimal charge time duration, minimal gassing and minimal temperature rise. This fast cycling procedure reduced gassing four times in comparison to the normal charge and significantly limited the drying out risk. Coulombic (Ah) efficiency was higher and the charge factor was lower at the fast charge in comparison to the normal charge cycling. Fully discharged battery can be charged to 80% SOC by already well optimized and tuned current step down fast charge in 30 minutes.

The fast charge usually recharges the battery to about 90% SOC for maintaining short charge duration. Regular full charge is very important in order to recharge the missing charge, to prevent undercharge degradation effects, and also to equalize individual cells SOC in the battery. Laboratory cycling was fitted to the real EV operation and necessary full recharge was performed regularly in the fast cycling procedure consisting of four fast charge (day time operation) and one normal charge (night time full recharge) consecutive cycles. Dynamic discharge ECE15L80%Pb specified by EUCAR and simulating electric vehicle discharge was used. The fast charge can properly utilize the charge acceptance of VRLA batteries and significantly increase performance of EV with limited driving range.

The new method for measurement and evaluation of current distribution over the electrode surface area was proposed and realized within this thesis. Results of the measured and analyzed current distribution at the fast charge indicate some important drawbacks that are significant for the cycle life! By this method worse current distribution was indicated for higher charge rates and the particular problem of the bottom part poor recharge was indicated. The alternative cell design of electrodes' lugs positions (top-bottom) would enhance the current distribution particularly at the fast charge.

Application of cells equalizing system was considered and found beneficial at the normal charge whereas at the fast charge it was found to be beneficial only for the final low current rates. This would minimize investment costs for an equalizer design. Individual cells voltage scattering

was found to be lower under higher charge rates when the individual cells voltages are dominated by kinetic overpotential rather then by internal resistance.

It was found that the fast charge had caused very significant corrosion protection of the positive electrode spines current collector system. The reason may be related to the positive electrode polarization. The positive electrodes' higher polarization at charge accelerate the corrosion process. The high polarization at the fast charge is however short in time and the corrosion is lower in comparison to the moderate long duration polarization of the normal charge. A hypothesis was proposed concerning the positive electrode discharge potential influence on the corrosion.

Basic crystallization principles say: higher current $\Rightarrow$ smaller crystals. Therefore smaller particles were expected to be measured at those fast charged cells. However the current distribution over the electrodes' surface area that was measured together with undercharging of the bottom parts have drastic influence to the particles size. The PAM from the electrode top part of the fast charged cell contained smaller particles in comparison to the normal charged cell! Particle size was analyzed by SEM and also by modern flow particle image analyze (FPIA) method. PAM agglomerates evaluated by laser diffraction seemed to be less stiff and less compact at the normal charge.

Porosity of the positive electrode is rising with cycle number. The fast charge forced moderate porosity increase in comparison to the normal charge. Negative electrode porosity had decreasing tendency at cycling and lower decrease was indicated for the fast charge. Higher acid stratification was measured at the fast charged cells. It is related to the higher charge rates and higher sulfation on electrodes bottom parts. This limits the fast charged battery performance at high power discharge.

The normal charge and the fast charge regime were also tested within this work in cycle life tests. Maximal cycle life result of the fast charged short cells string series was about 40% longer in comparison with the normal charged series, achieving 930 and 670 cycles respectively. These cycle life results belong in both tests to the strongest cell of those series and to the constant current C/2 rate discharge. Cycle life tests of series connected blocks were done by the dynamic ECE15L80%Pb discharge. The fast cycling cycle life was measured approximately 470 cycles. The cycle life benefit in comparison to the normal cycled blocks series can be correctly considered in the range of 10 to 20%.

At the end of blocks series cycle life individual blocks performance were found to be the most homogeneous at the fast cycled string. After the cycling, capacity scattering at individual cells within blocks always indicated the middle cell as the weaker cell, while those cells in the block side positions expressed the highest capacity. When the weakest cell was not considered, the highest homogeneous end of discharge voltages were detected at the block from the fast cycled string. At all blocks series cycling the positive electrode was found to be limited, however the best state of the positive electrode was indicated at the fast cycled blocks string.

After opening of cells from the normal charged battery those positive tubular electrodes seemed to be mechanically softer and separators seemed to be drier compared to the fast charged battery.

Results of those analysis are so favorable for the fast charge that much longer cycle life benefit would be expected. However, as was mentioned the irreversible sulfation particularly at the electrodes' bottom part of those fast charged cells including acid stratification were more intensive comparing to the normal charge. That unfortunately contradicts those beneficial effects and the cycle life prolongation is not so revolutionary.

Different <u>dominating</u> degradation effects were found for the normal and for the fast charge. **The dominating degradation effects of the fast cycled cells seems to be the irreversible sulfation together with acid stratification and the worse current distribution forcing intensive degradation of the electrodes' bottom parts. At the normal cycled cells the dominating degradation effects seems to be the positive electrode current collector corrosion reducing properties of PAM-current collector interface together with structural-properties degradation changes of the bulk PAM.**

Despite not so revolutionary cycle life prolongation at the fast charged thin tubular VRLA battery, there may be very clear and important statement that **the current step down fast charge does not harm these batteries**. The current step down fast charge was proved to be excellent and reliable charge regime for VRLA batteries. Battery overall gassing was reduced as well as average charge factor, columbic (Ah) efficiency was increased. The new developed thin tubular VRLA battery and the current step down fast charge procedure are well suited for EV applications.

Hints for further research:
Further investigations may concern on the alternative electrodes' lugs design and current distribution. Evaluation of the current distribution over the electrode area should be measured in VRLA sealed conditions.

The hypothesis concerning the positive electrode spines current collector corrosion dependence on the positive electrode potential at discharge should be proved and tested. The influence of the fast charge on the positive electrode potential at discharge should be also studied.

REFERENCES

[1] Harbolla B.: Analysis of hybrid drive systems with new electric components: morphology, evaluation and optimization., Summary report, RWTH, EDS project, VVERE contract P-030, EU - contract TEAE-CT88-0001, Dec. 1992

[2] Grand project GA/1038/94 1996, CITYCAR SYSTEM, Ministry of Environment, Czech Republic

[3] Bullock K.R.: The advancing lead-acid battery, Advances in lead-acid batteries, Proceeding volume 84-14, The Electrochemical Society, Pennington, NJ, USA, 1984

[4] Garche, J.: Corrosion of lead and lead alloys: influence of the active mass and of the polarization conditions, J. Power Sources 53 (1995) 85-92

[5] Atlung S.: Failure mode of the negative plate in recombinant lead/acid batteries, J. Power Sources 52 (1994) 201-209

[6] Specification of Test Procedures for Electric Vehicle Transportation Batteries, EUCAR Traction Battery Working Group, Dec. 1996

[7] Lander J.: Further Studies on the Anodic Corrosion of Lead in H_2SO_4 Solution, J. Electrochem. Soc., Vol. 103, No. 1

[8] Ekdunge P., Simonsson D.: Kinetic and structural changes of the porous lead dioxide electrode during charge, Advances in lead-acid batteries, Proceeding volume 84-14, The Electrochemical Society, Pennington, NJ, USA, 1984

[9] Kordesch K.V.: Charging method for batteries, using the resistance free voltage as endpoint indication, J. Electrochem. Soc., 113 (1972) 1053

[10] Nor J.K.: EP Patent No. 0 311 460 A2, (Oct. 10, 1988)

[11] Nor J.K.: US Patent No. 5 202 617, (Apr. 13, 1993)

[12] Regner A.: Technicka elektrochemie 1, Academia, Praha 1967

[13] Bard J.A.: Electrochemical methods, John Wiley & Sons, Inc. 1980

CURRICULUM VITAE

Ing. Vojtěch SVOBODA, Ph.D.
Narozen: 23. 4. 1973 v Brně.

Studium:
1996 dokončeno inženýrské studium na FEI VUT v Brně v oboru:
26-33-8 Silnoproudá elektrotechnika a elektroenergetika *(dne 10.7.1996 na téma Nastavení distanční ochrany transformátoru zálohující odchozí vedení z rozvodny 110 kV)*
V průběhu studia na VUT Brno odborné praxe v USA, Finsku a Portugalsku. Předseda mezinárodní studnetské organizace IAESTE na VUT Brno.
1996 – 1999 interni doktorand na UETE FEI VUT v Brně

V roce 1996 zahájeno na VUT Brno Doktorandské studium. Praktická a experimentální část Doktorandské práce byla zpracována v ZWS Ulm v SRN.

2002 dokončeno doktorské studium v oboru:
P 2643 Elektrotechnika, elektronika, komunikační a řídící technika
ve studijním oboru Mikroelektronika a technologie na Fakultě elektrotechniky a komunikačních technologií, VUT v Brně

ABSTRAKT

Disertační práce popisuje princip olověného akumulátoru. Nové VRLA trakční akumulátory, s tenkými trubkovými kladnými elektrodami, byly vyvinuty a vyrobeny ve firmě CMP Exide Ltd. ve Velké Británii. Konstrukční řešení vhodně kombinuje výhody odolných robustních kladných trubkových elektrod s vylepšenými výkonovými parametry velmi tenkých elektrod. Použité VRLA akumulátory měly nominální kapacitu 70Ah, 3.5mm tenké kladné trubkové elektrody a AGM separátory. Byly vyrobeny ve formě jednotlivých článků a 12V bloků. Akumulátory těchto typů byly použity ve všech, v práci uvedených experimentech.

V této práci jsou diskutovány a řešeny dvě nabíjecí metody: Normální nabíjení I-U-I a nově vyvinuté rychlé nabíjení se skokově se snižujícím proudem. Tato unikátní procedura rychlého nabíjení dovoluje nezávislé nastavení proudových a napěťových parametrů v jednotlivých stupních konstantního nabíjecího proudu. Jedná se o velmi univerzální, adaptibilní a výkonnou nabíjecí metodu. Tato metoda rychlého nabíjení byla, při zohlednění mnoha parametrů, optimalizována a vyladěna pro krátký nabíjecí čas a pro minimální opotřebovávání testovaných VRLA baterií.

Chování sériově a paralelně zapojených článků bylo zkoumáno pro oba druhy nabíjení. V rámci této disertační práce byla navržena a realizována nová experimentální metoda pro hodnocení proudového rozložení na povrchu elektrod při nízkých a vysokých proudech. Získané výsledky byly vyhodnoceny a prokázaly, že při nižším nabíjecím proudu je lepší homogenita rozložení proudu na povrchu elektrod. Bylo prokázáno, že u rychlého nabíjení se vyskytují problémy při nabíjení spodních částí elektrod, což vede k jejich nevratné sulfataci.

Cyklová životnost byla testována a vyhodnocena u samostatných článků, sériově zapojených článků a u sériově zapojených 12V bloků pro oba nabíjecí režimy. U sériově zapojených bloků byla použita dynamická vybíjecí procedura ECE15 simulující jízdu elektrického vozidla. Rychlá nabíjecí metoda může prodloužit životnost akumulátorů, avšak reálné prodloužení životnosti lze očekávat spíše kolem 10% než 40%. Prodloužení cyklové životnosti o 40% bylo naměřeno u krátké série jednotlivých článků.

Po skončení životnosti byly provedeny různé testy cyklovaných akumulátorů; následné detailní analýzy byly provedeny za účelem nalezení a specifikování dominantního degradačního procesu. U normálního a u rychlého nabíjení byly zjištěny odlišné dominantní degradační efekty. Procesem dominantní degradace u rychle nabíjených akumulátorů byla vyhodnocena nevratná sulfatace, stratifikace elektrolytu a zhoršená proudová distribuce ve spodní části elektrod. Procesem dominantní degradace u normálně nabíjených akumulátorů byla vyhodnocena koroze kladných elektrod a disintegrace kladné aktivní hmoty.